C3 Final Showcase Report

Paytn Barnette, Paul Brich, Chanel Davis, Connor Hall, Brendan King,

Bruce Noble, Parker Scribner, and Lawrence Tolentino

Embry-Riddle Aeronautical University, Prescott, AZ, USA

The Mission for Orbital Servicing and Support (MOSS) is a satellite servicing architecture developed to extend the operational lifetime and capability of geostationary orbit (GEO) spacecrafts. MOSS integrates two servicing payloads, the Core Orbital Refueling Kit (CORK) and the Solar Panel Augmentation Reflector Kit (SPARK), to address the primary drivers of satellite end-of-life: propellant depletion and power degradation. The system operates as a hosted payload on the ESPAStar platform and performs autonomous docking, fluid transfer, and deployable power augmentation. System architecture, concept of operations, and subsystem-level analyses demonstrate feasibility through structural validation, fluid-system design, and autonomous-control implementation. Cost analysis indicates that MOSS provides significant savings compared to full satellite replacement by targeting only depleted subsystems.

Nomenclature

CFD = Computational Fluid Dynamics

CORK = Core Orbital Refueling Kit

ES&A = Electrical, Software, and Autonomy

FEA = Finite Element Analysis

GEO = Geostationary Orbit

M&S = Mechanical and Structural

MOSS = Mission for Orbital Servicing and Support

SPARK = Solar Panel Augmentation Reflector Kit

STP = Standard Temperature and Pressure

TRL = Technology Readiness Level

I. System Overview

THE Mission for Orbital Servicing and Support (MOSS) is a satellite servicing architecture developed to extend the operational lifetime and capability of geostationary orbit (GEO) spacecraft. MOSS integrates two servicing systems, Core Orbital Refueling Kit (CORK) and Solar Panel Augmentation and Reflector Kit (SPARK), which address the primary limitations of satellite end-of-life: propellant depletion and power degradation. The system is designed to operate without requiring pre-existing servicing interfaces, enabling compatibility with current on-orbit assets. Through a combination of autonomous docking, fluid transfer, and deployable power augmentation technologies, MOSS provides a scalable approach to sustaining high-value space systems. This section presents the system architecture, concept of operations, and the driving problem and mission impact that define the overall desi

.

A. System Architecture

For the overall goal of Mission for Orbital Service and Support (MOSS), two servicing missions were derived: Core Orbital Refueling Kit (CORK) and Solar Panel Augmentation Reflector Kit (SPARK).

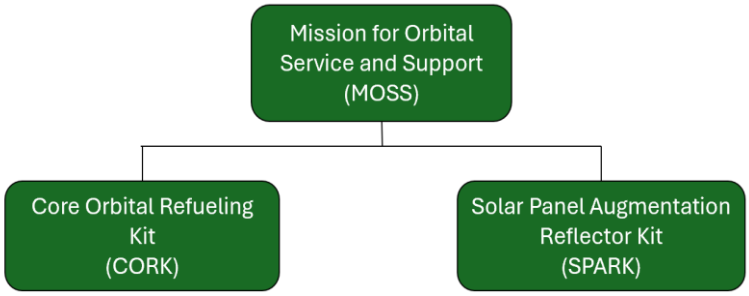

Fig. 1 MOSS System Architecture

CORK aims to refuel GEO satellites. Specifically, those using a monopropellant hydrazine-based propulsion system. This is because monopropellant hydrazine is the most common type of propulsions from a survey of currently active satellites in September 2025. SPARK aims to revitalize degraded solar panels, by increasing the solar flux received by the solar panel, using reflectors.

1. *MOSS Concept of Operations*

A storyboard has been created to outline the mission timeline. This storyboard is shown in Fig. 2 below.

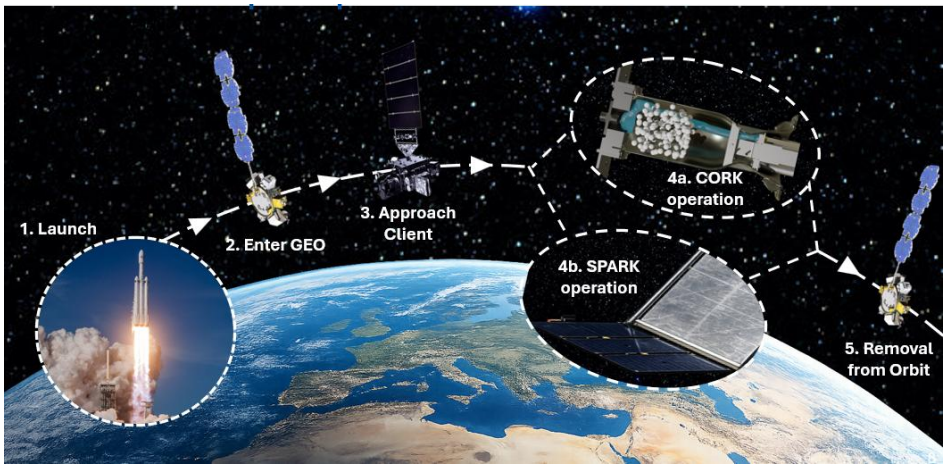

Fig. 2 MOSS Concepts of Operations

The MOSS mission will have 5 steps of operation. Within step 4 there will be two possible sequences of events based on whether CORK or SPARK is being deployed.

Phase 1 encompasses the launch of the system. The MOSS system containing CORK and SPARK will utilize the ESPAStar platform. The entire system will be launched aboard a Flacon Heavy launch vehicle.

In Phase 2, the system will be transferred to a geostationary orbit, as GEO client satellites are the main target of the MOSS system.

In Phase 3, the system approaches the targeted client satellite and proximity operations are performed. This allows the MOSS system to get close to the client satellite to perform docking and service operations.

In Phase 4a (CORK Operations), the system aligns with the designated interface then establishes a secure mechanical connection by inserting and sealing to the engine nozzle. The system then activates the primary functional mechanisms, preparing for propellant transfer. CORK then performs propellant backflow of monopropellant through the client satellite's engine and into its propellant tank. The attached sensors ensure safe and complete propellant transfer. Following completion of operations, CORK vents residual propellant, disengages from the client satellite.

In Phase 4b (SPARK Operations), the system aligns with the designated interface then establishes a secure mechanical connection by clamping onto the solar panel structure. The system then activates the primary functional mechanisms, preparing for power augmentation. SPARK then deploys a tape-truss-supported reflective surface along the length of the panel. The aluminized film reflector is positioned to redirect additional sunlight onto the client satellite's solar array, increasing incident solar flux and improving power generation capability. After deployment SPARK remains attached as a passive augmentation device.

Phase 5 encompasses the disposal operations of the system. After CORK disengages from the client it will depart for disposal or relocation to a graveyard orbit. Since SPARK is a passive augmentation device, it will remain with the client spacecraft and will be disposed of with the host spacecraft.

2. *Driving Problem and Impacts of Mission*

The space industry is both costly and rapidly expanding, with GEO satellites costing $500M USD or more to manufacture and launch [1]. Satellites are designed for unique missions, and inactive satellites must be replaced with newly built ones. The Space Report 2023 Q4 stated, “more than 2,800 satellites deployed into orbit, 23% more than in 2022” [2], highlighting the increasing demand for replacement and additional satellites. However, satellites at the end of life often still contain functioning hardware, as their lifespans are limited by propellant capacity [3] [4]. Depleted propellant means the end of the mission, even though only the propellant caused the retirement. On-orbit refueling targets the propellant system, mitigating the cost of manufacturing new satellites. CORK addresses this by enabling refueling of existing satellites that lack a refueling interface.

Power generation is another critical limitation for GEO satellites. Solar panels degrade over time due to radiation, thermal cycling, micrometeoroid impacts, and material aging, reducing available power and limiting mission capability. Although many satellites remain structurally and functionally intact, reduced power can prevent full mission operations, leading to inefficiencies and early retirement of useful spacecraft. SPARK addresses this by increasing the sunlight directed to existing solar arrays, improving power generation, and offsetting degradation.

B. Feasibility of Mission

MOSS is a complete design due to manufacturability, technology cost, and readiness. Manufacturability is supported by available components and flight-proven materials. CAD models for CORK and SPARK have been developed to part-level detail, and the system can be manufactured and tested within five years or less.

The technology readiness level ranges from TRL 3 to TRL 6. Gaps include catalyst cooling, composite layup, and clamp testing. Preliminary analysis and subsystem-level validation demonstrate that the system is capable of meeting mission requirements. These gaps can be addressed through ground testing and do not limit mission feasibility.

Using NASA’s Advanced Mission Cost Model, the total mission cost is $231.81 million (FY 2026), including production, integration, and launch. Compared to the $373.63 million cost of GOES-P replacement, MOSS provides

$141.82 million in savings. This reduction is driven by lower system mass and reduced mission complexity, as MOSS replaces only depleted subsystems rather than the entire spacecraft.

II. Cork Design and Analysis

The Core Orbital Refueling Kit (CORK) is a servicing payload designed to extend the operational life of GEO satellites by enabling on-orbit refueling through existing engine nozzles. CORK performs autonomous docking, sealing, and controlled propellant backflow without requiring pre-existing refueling interfaces. CORK's ability to backflow propellant enables on-orbit servicing with current on-orbit assets. CORK provides a scalable and feasible approach to mitigating propellant depletion, the primary driver of satellite end-of-life.

C. Cork System Architecture

To ensure the achievement of all proposed service goals, requirements were developed to address all critical considerations. These requirements are included in further detail in Table 1.

Table 1 CORK System-Level Requirements

ID	Description	Verification	Satisfied
R1.1	CORK shall **backflow propellant** through MONARC 22-12LT+HT thruster.	Simulation, Testing	Future Work
R1.2	CORK **shall not damage** GOES-R**.**	FEA	Future Work
R1.3	CORK shall **terminate** the propellant transfer **autonomously**.	Software Design	Yes
R1.4	CORK shall **determine** when the **transfer has been completed**.	Software Design	Yes
R1.5	CORK shall **seal against the** MONARC 22-12LT+HT thruster.	Testing	Future Work
R1.6	CORK shall fit within stowage dimensions of ESPAStar payload bay.	Mechanical Design	Yes
R1.7	CORK shall be operational within ESPAStar's power capabilities of 200W.	Electrical design	Yes
R1.8	CORK shall mass less than 320kg.	Mechanical Design	Yes

A prototype of the CORK was designed and manufactured for testing on the Embry-Riddle Aeronautical University Campus. The engine used for testing is referred to as Janus-R. All diagrams and analysis were calculated using Janus R to show requirements can be analyzed, tested, and met. All analysis can be repeated on various client

structures to ensure success and repeatability for the full-scope mission. As such similar analysis will be conducted on the MONARC 22-12LT+HT thruster and GOES-R to fully meet the system requirements shown in Table 1.

To meet all requirements, the CORK system was designed with three primary subsystems: Mechanical and Structural, Fluids, and Electrical, Software, and Autonomy. Each subsystem has specific subsystem requirements to ensure the fulfillment of the overall system-level requirements.

D. Mechanical and Structural Subsystem

The Mechanical and Structural (M&S) subsystem encompasses the hardware present in the operation of the CORK design. The system includes a docking mechanism to latch to the client to be refueled, and a sealing surface which is clamped via the docking interface to create a full seal to allow fluid transfer.

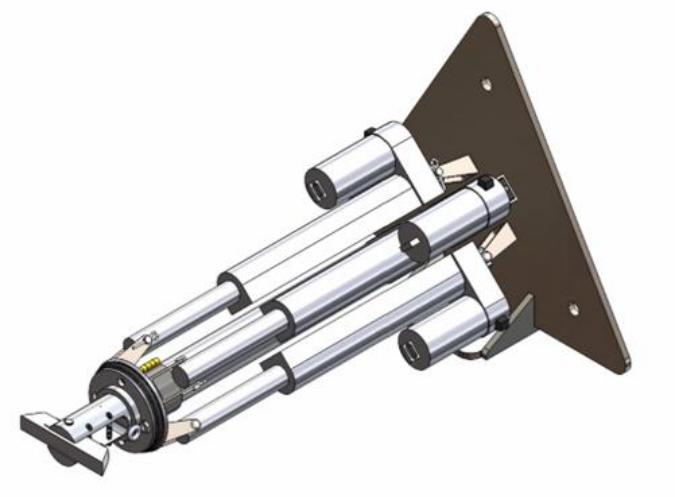

Fig. 3 CORK Mechanical Subassembly

The CORK mechanical subassembly consists of three lower subassemblies, accumulating a total of 76 components. CORK makes use of linear and rotational motion to dock and seal against the client engine, applied by a torsion spring and linear actuators on the main assembly.

3. *Accessing and Docking*

The process of accessing and docking is conducted using a rotating grapple foot, which is attached to the plug using a tension lanyard and torsion spring, seen in Fig. 4. When coupled with the movement of the Plug, this creates two default states for CORK; extended and retracted.

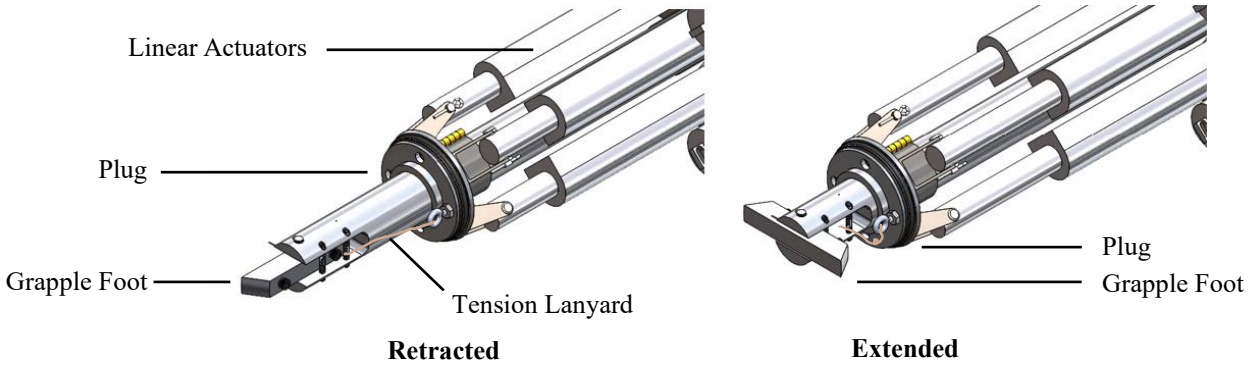

Fig. 4 Grapple Foot and Plug Actuation

Shown in Fig. 4, the Plug translates axially toward and away from the nozzle using linear actuators with a lanyard, coupling its motion to the grapple foot. This approach minimizes the complexity of the system and potential modes of failure. This approach allowed MOSS to create a slimmer body to pass through the nozzle. CORK rotates the Grapple Foot to reduce the cross-sectional profile of the body, enabling it to pass through the throat of the nozzle, as seen in Fig. 5.

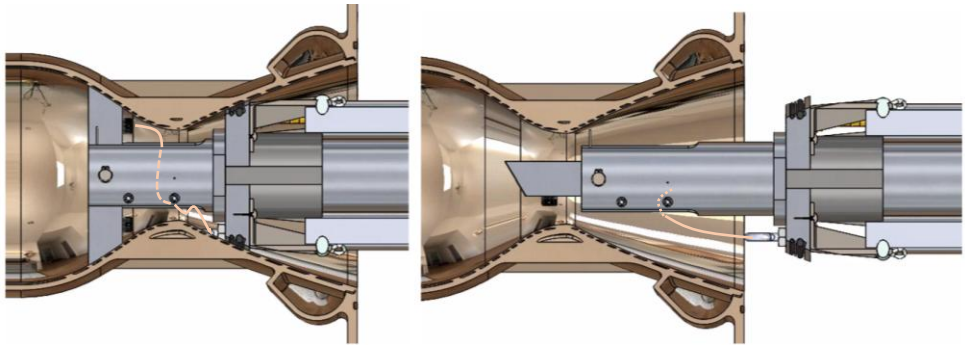

Fig. 5 CORK and Janus R docking

Fig. 5 is a section cut from the centerline of Janus R. The pivoting of the grapple foot and contact from the plug locks CORK into the Janus R chamber. To meet all requirements pertaining to docking, tests will need to be conducted to verify the design. Those tests, including hydrostatic proof tests, low pressure leak checks, and operational transfer tests, these will occur in 2026.

4. *Sealing*

CORK uses the plug subassembly shown in **Error! Reference source not found.** to seal against pressure inside the chamber. The system consists of three O-rings to eliminate leaks. Analysis was conducted using manufacturer tools from the Parker corporation to select the O-rings used on the plug to seal against the load bar and Janus R [5].

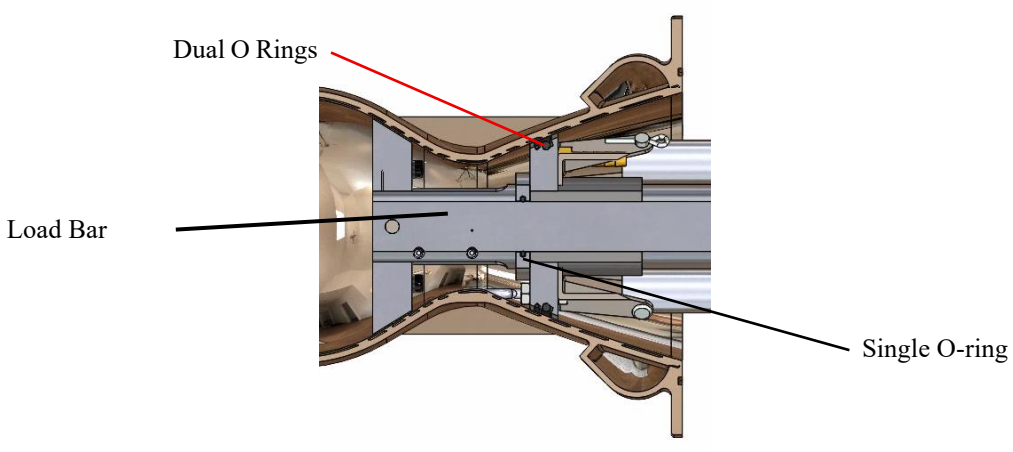

Fig. 6 Sealing CORK

In Fig. 6 above it shows that a single inner O-ring is used to seal against the load bar, while two outer O-rings are used to seal against the Janus R chamber. The surface of the Janus R nozzle is rough because of the laser sintering process used to manufacture the engine. This rough surface produces a particular challenge for leak mitigation, which is why MOSS has opted to include two O-Rings on the plug subassembly. The two O-Rings will not only assist with the sealing capabilities for Janus R, but many other nozzles as well. In the full-scope mission multiple nozzle geometries will be serviced, the dual O-Rings will offer redundancy to ensure proper sealing for these various geometries.

5. *Damage Control*

To ensure no damage will be done to the Janus R chamber, Finite Element Analysis (FEA) of a section of the chamber was conducted. Janus R features complex regenerative cooling channels that complicate the structural analysis of the chamber. Fig. 7 shows the intricate geometry and thin wall size due to the regen pathways in the chamber.

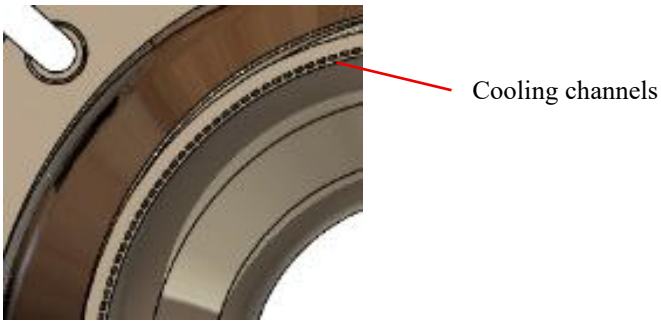

Fig. 7 Janus R Regenerative Cooling Channels

The analysis was focused on a singular section due to the thinnest structure and highest stress location, where the foot contacts the regen channels. If the cooling channels' thin walls were to be punctured this would form a leak in the Janus R chamber. The analysis was done on the area of contact the CORK foot has with Janus R to increase accuracy of results due to limited meshing size during FEA. Results of the section cuts FEA are seen in Fig. 7.

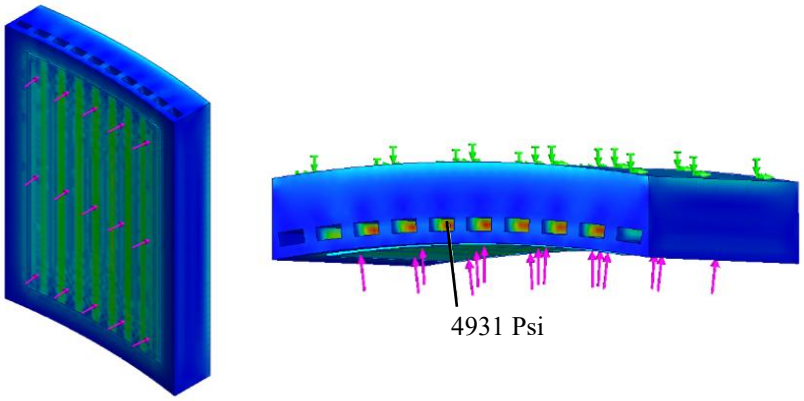

Fig. 8 FEA of worst-case load applied to Janus R foot contact area

FEA results shown in Fig. 8 show a maximum load inside the regen walls of 4931 Psi. The chamber, made of Inconel 718 has a yield stress of 180,000 Psi [6]. CORK's simulated stress is within yield stress by a factor of safety of 36. Ultimately, due to Janus R being constructed out of Inconel 718, there is little concern for damage to Janus R, the grapple foot is expected to break before damaging the chamber.

6. *Mechanical Subsystem Analysis*

CORK requires additional analysis separate to the analysis of Janus R to verify the MOSS-designed mechanical structure of CORK can withstand the loads experienced during nominal operation. Of these parts, the most concerning were the dowel pin and grapple foot, seen in Fig 9.

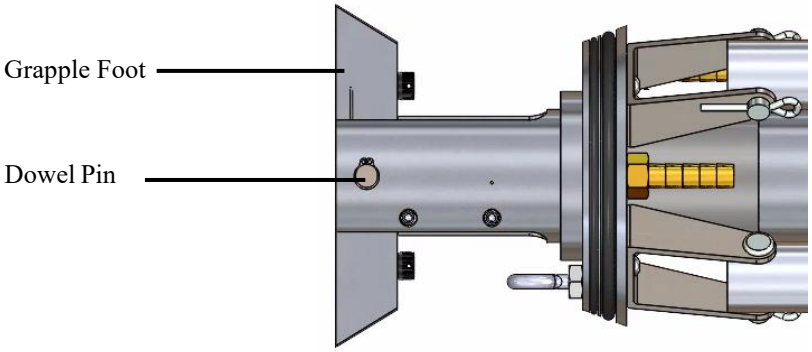

Fig. 9 High Stress Components on CORK

MOSS chose the grapple foot, dowel pin, and a few other components to focus on because they bear the highest loads on the system. Component failure in these locations would damage other components of CORK and cause the seals between CORK and Janus R to fail. To combat this, MOSS conducted FEA on the grapple foot and dowel pin; results of this analysis are visible in Fig. 10

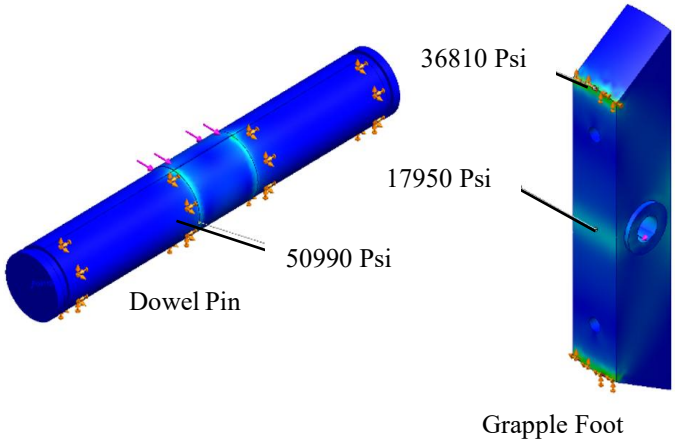

Fig. 10 Peak stress locations on dowel and foot

Before selecting materials, the simulated stresses in each part were evaluated. The dowel pin must withstand the full reaction load transferred through the grapple mechanism. The grapple foot must resist the primary bending load around the dowel-pin hole. A worst-case scenario contact load was applied directly to the leading edge of the wedge to simulate the condition where bending causes the edge to take the full reaction force. A factor of safety much greater than 1 is not required for this edge case, as yielding here would only round the leading edge and would not cause a full part failure.

With the required loading established, the resultant maximum stress in the dowel pin was found to be 50,990 Psi, as shown in Fig. 10. To maintain a large factor of safety for this crucial part, a material well above the simulated stress was required. The dowel pin will be machined from 13-8 H1025 stainless steel. An average yield strength above 185,000 Psi provides a factor of safety of at least 1.5 under the maximum predicted load [7].

For the wedge, FEA produced a maximum stress of 36,812 Psi at the leading edge and 17,950 Psi at the dowel-pin connection hole shown in Fig. . The true design driving load is the bending stress at the dowel-pin hole and not the edge contact load, AL 6061-T6 was selected. Its yield stress of 40,000 Psi [8] provides a factor of safety above 1.5 at the critical dowel-pin hole location, and a smaller but acceptable factor of safety at the worst-case edge load.

These results, along with the chosen materials, indicate that CORK is a structurally feasible design and is capable of safely transferring propellant.

E. Fluids Subsystem

The fluids subsystem encompasses all components related to refueling client satellites in addition to research regarding propellant and catalyst interactions. The major fluid subsystem components include CORK's propellant tank, the catalyst, and plumbing and instrumentation to connect the two tanks.

7. *CORK Propellant Tank*

CORK will have two propellant storage tanks integrated onto ESPAStar to enable on-orbit refueling. The propellant tanks will regulate the transfer pressures keeping them within safe operating limits. This ensures compatibility with existing satellites' hardware. The system will utilize the onboard ESPAStar propellant tank in conjunction with two auxiliary tanks, all connected within a single integrated fluid system to provide sufficient storage capacity and maintain controlled, continuous flow during backflow operations.

8. *Bypassing the Catalyst to Backflow Propellant*

In hydrazine monopropellant thrusters, catalysts decompose hydrazine to produce thrust. For backflow refueling, the catalyst must be bypassed to avoid hydrazine decomposition. During backflow operations, interaction between the catalyst and hydrazine is unavoidable. However, without mitigation, the catalyst would decompose a significant portion of the propellant before it reaches the client's propellant tank. Therefore, research on methods to bypass the catalyst by decreasing the reaction rate with hydrazine was performed.

Hydrazine is typically stable at room temperature but will decompose rapidly in the presence of a suitable catalyst, producing significant of heat and pressure. For MOSS' backflow operations, this is not ideal since heat and pressure buildup in the client's internal fluid system without relief will lead to structural failure. To avoid potential failures, the hydrazine catalyst must be bypassed when backflowing hydrazine through an engine.

A main challenge is that hydrazine catalysts are typically paired with internal heaters to maintain temperatures that produce more efficient hydrazine decomposition. Hydrazine catalysts are sensitive to temperature and are shown to have degraded performance under cold conditions. By lowering the temperature from around 50 ºC to 23 ºC (3.1 to 3.3 x 10^3 $^oK^{-1}$), reaction rates decrease by 1 to 2 orders of magnitude based on the catalyst type [9].

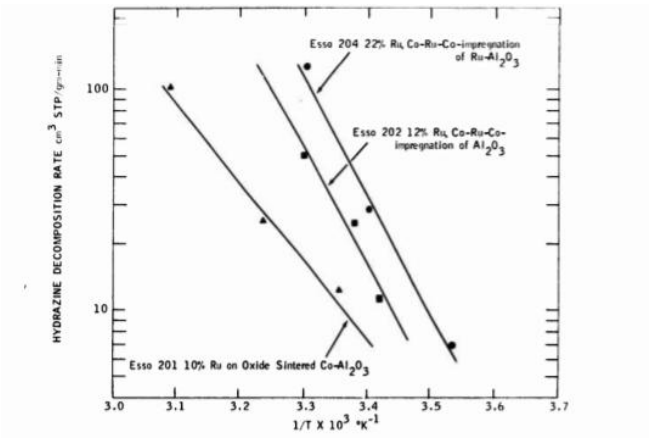

Fig. 11 Performance of Monopropellant Catalysts as Temperature Varies [9]

High reaction rates are directly proportional to high hydrazine decomposition rates. ESSO 201 and ESSO 202 have lower reaction rates at this temperature such as 10 and 25 $\frac{cm^3(STP)}{min*gram}$. These catalysts are more sensitive to temperature, causing a larger performance loss when temperature is not maintained. Therefore, CORK will focus primarily on refueling satellites that have ESSO 201, ESSO 202, or similar sensitive catalysts to minimize the hydrazine decomposition rate as propellant backflows through the engine.

Servicing will only be done to satellites with temperature sensitive catalysts and at low temperatures. A CFD analysis is in-progress and will be used to further analyze the effects of hydrazine decomposition and catalyst bed interactions during MOSS' refueling operations. The goal of the CFD analysis will be to verify the assumption that MOSS will be able to bypass the hydrazine catalyst.

9. *CFD Analysis on Catalyst Bypass*

A CFD model was created in ANSYS Fluent to analyze the complex reactions between hydrazine and a catalyst bed. CFD models in this area of research were promising however there was no data on large amounts of liquid hydrazine flowing over a catalyst bed as this would never happen in forward flow hydrazine thruster process. As such, a CFD model by Mughari et. al. that analyzed the forward flow of hydrazine was reproduced and augmented to incorporate multiphase backflow of hydrazine across a catalyst bed [10].

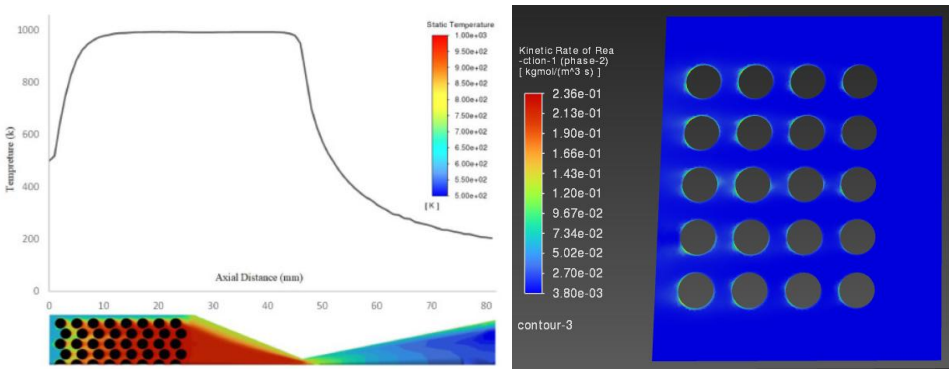

Fig. 6 Side-by-side comparison of Mughari et. al. CFD model (left) versus MOSS CFD model (right)

The MOSS CFD model is a quasi-2D mesh of the straight portion of the decomposition chamber of a 20N hydrazine monopropellant thruster. The main sub-models of the CFD model are multiphase model, turbulence model, and 1-step surface reaction model driven by Arrhenius rates. The extended feature list of the model is listed in Fig 13.

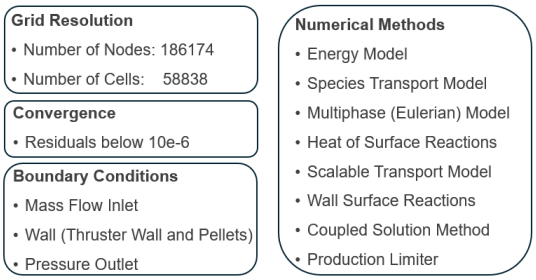

Fig. 73 List of MOSS CFD model details

From the use of the model, analysis was conducted to determine if liquid hydrazine could backflow over a catalyst bed without causing thermal runaway in addition to characterizing how the hydrazine decomposition reaction rate varies with respect to the temperature and mass flow rate of the liquid hydrazine.

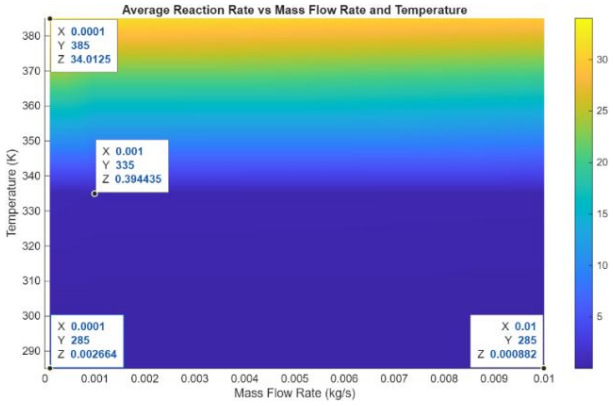

Fig. 84 Average Hydrazine Decomposition Reaction Rate vs Mass Flow Rate and Temperature of Hydrazine

Preliminary results indicate that the average hydrazine decomposition rate decreases as the temperature decreases and mass flow rate increases. Fig. 14 shows a surface plot of 12 CFD run results of various temperature and mass flow rate initial conditions with linear interpolation between the points. Thermal runaway was also not observed in any of the CFD model runs which supports that the backflow of hydrazine can occur without damaging a client satellite. Experimental research is desired to further understand the intentional full liquid hydrazine flow over a catalyst bed.

F. Electrical, Software, and Autonomy Subsystem

The Electrical, Software, and Autonomy system (ES&A) contains the mechanisms that control the flow of the propellant. CORK must be autonomous, requiring a monitoring system to determine the condition of the transfer. Implementation of autonomous monitoring and control was broken into two tasks. First, CORK must track the total amount of propellant to ensure a complete transfer. Second, there must be valves to start and stop the flow of fluid.

The goal of monitoring the propellant transfer is to measure the transfer rate and determine when the transfer is complete. A Hall-effect flow sensor measures volumetric flow rate, which is integrated over time to calculate the total volume transferred. Once the required volume is reached, a signal is sent to terminate the transfer. This method assumes no leaks, so pressure transducers are used to verify that system pressure remains constant. One transducer is placed in the tank, and another is placed before the outlet to Janus R. If a large pressure drop is detected, indicating a leak, a termination signal is sent to prevent propellant loss and inaccurate measurements.

The goal of controlling the transfer is for the system to start upon human input and stop upon human or sensor input. The solenoid valves are computer activated after operator input. The system runs until the transfer is complete or an error is detected, at which point power is stopped to terminate the transfer. An operator can also stop the system using an emergency shut-off switch to safely depressurize. This electronics plan satisfies the requirements needed for mission completion.

G. CORK Risk Mitigation

CORK risks are driven by high-pressure fluid transfer, system control, and client interaction. Pressure failures are mitigated through structural sizing and relief valves to maintain safe operating limits. Loss of power results in a fail-safe system where valves close and flow stops. Mechanical damage to the client is mitigated through load analysis to ensure forces remain within allowable limits. Catalyst reaction risks are reduced by controlling flow rate and propellant temperature, preventing over-pressurization and thermal damage.

III. SPARK design and analysis

The Solar Panel Augmentation Reflector Kit (SPARK) is a servicing payload designed to extend the operational capability of GEO satellites by increasing available electrical power through solar augmentation. SPARK attaches to existing solar arrays and deploys a lightweight reflective system to redirect additional sunlight onto the panel without modifications to the spacecraft. The system integrates clamp, deployment, and reflector subsystems to ensure secure attachment, controlled deployment, and effective light redirection while maintaining structural integrity and meeting constraints on volume, mass, and power. Through this architecture, SPARK provides a scalable and non-invasive approach to mitigating power degradation and enhancing on-orbit performance.

H. SPARK System Architecture

To ensure the achievement of all proposed service goals, requirements were developed to address all critical considerations. These requirements are included in further detail in Table 2.

Table 2 SPARK System-Level Requirements

ID	Description	Verification	Satisfied
R1.1	SPARK shall **reflect an additional 11% of light** from the sun onto the solar panels.	Analysis	Yes
R1.2	SPARK shall **increase station keeping burn time** within **5%.**	Analysis	Future Work
R1.3	SPARK shall **not break client solar arrays during maneuvers.**	Analysis	Future Work
R1.4	SPARK shall mount in a way that **does not damage client** solar cells.	FEA	Future Work
R1.5	SPARK shall **fit within stowage dimensions** of ESPAStar Payload bay.	Mechanical Design	Yes
R1.6	SPARK shall be operational within ESPA stars **Power capabilities of 200W.**	Electrical Design	Yes
R1.7	SPARK shall mass **less than 320kg.**	Mechanical Design	Yes

To meet all requirements, the SPARK system was designed with three primary subsystems: Clamp Subsystem, Deployment Subsystem, and Reflector Subsystem. Each subsystem has specific subsystem requirements to ensure the fulfillment of the overall system-level requirements.

10. *Clamp Subsystem*

The clamp subsystem provides the mechanical interface between SPARK and the client solar panel. The clamp's primary function is to securely attach the system onto the solar panel. To satisfy the overall mission requirements, implementation of the clamp subsystem was driven by three primary goals. First, it must ensure a secure attachment to the client panel is made. Second, it must remain within an acceptable mass budget to support spacecraft integration constraints and reduce changes in the moment of inertia of the spacecraft. Third, it must attach without causing structural or surface damage to the panel.

To maintain compatibility with the client solar panel the clamp must minimize minimizing interference with active solar cells while maintaining secure attachment to the panel. The contact area is limited to less than 6 square inches to avoid blocking solar flux. CAD layout and dimensional verification were used to ensure that clamp contact points align only with allowable attachment regions, preventing interference with solar energy generation.

To remain within an acceptable mass budget, the clamp subsystem is constrained to a total mass of 10 kg or less. Mass efficiency was a primary driver during material selection and structural sizing. Components were minimized where possible while maintaining sufficient stiffness and strength for secure attachment. Analytical mass estimation and CAD-based mass property evaluation were used to verify compliance with the allowable limit, demonstrating that the clamp satisfies both structural and system-level mass constraints.

To securely attach without damaging the client spacecraft, the clamp was designed to distribute load across appropriate structural contact regions rather than concentrating force at a single point. Contact surfaces are shaped to reduce local stress and avoid puncture, cracking, or deformation of the panel. Structural simulations evaluated clamp loading and verified that expected contact forces remain within allowable limits for the panel interface. This ensures secure attachment while preserving the integrity of the solar panel throughout operation.

Overall, the clamp subsystem design satisfies the primary structural and interface requirements needed for SPARK operation. Through geometric compatibility, lightweight construction, and non-damaging attachment behavior, the clamp provides a feasible method for securely mounting the system to a client spacecraft solar panel.

11. *Deployment Subsystem*

The deployment subsystem extends the reflective film from its stowed configuration to its fully deployed position, ensuring controlled and uniform deployment of the reflector. To satisfy the overall mission requirements the deployment subsystem was driven by 3 primary goals. First, the system must deploy the reflective film to a distance

that achieves the required optical performance. Second, it must remain within a constrained mass budget to support spacecraft integration. Third, it must provide uniform deployment using a simple and reliable actuation method. Lastly, the system must prevent damage to reflective film during deployment and operation. SPARK in a partially deployed out state is shown in Fig. 15.

Fig. 95 SPARK Deployed to a Length of 1 Foot

To achieve sufficient reflector coverage, the deployment subsystem extends the reflective film using a tape-truss deployment mechanism to a baseline distance of 3 meters. This length was selected to provide adequate reflective surface area to meet power augmentation requirements while remaining within packaging and structural constraints of the ESPAStar platform. Although the current configuration supports up to 3.49 meters based on CAD, the tape-truss design is inherently scalable and can be extended further if additional reflective area is required. This allows the reflective film to be unrolled in a controlled manner. Deployment simulations were conducted to verify that the reflector extends to the required distance while maintaining proper alignment with the solar panel. Results confirmed that the system achieves full deployment to the required length, ensuring a reflective surface area that meets power augmentation goals.

To ensure uniform and reliable deployment, the deployment subsystem will use a single motor to ensure even deployment of the reflective film. The system was designed with a centralized motor coupled to both tape truss deployment mechanisms that evenly distributes motion across the reflector. This approach eliminates synchronization issues that could arise from multiple actuators and reduces system complexity. Simulation of the deployment process confirmed that the reflector extends uniformly without skewing or uneven tension, verifying that the subsystem meets the requirement for controlled and consistent deployment.

To maintain a lightweight system, the deployment subsystem will have a total mass of 5 kg or less. The proposed design prioritized lightweight materials and compact mechanical components. The use of a single motor and simplified

transmission system minimized additional hardware mass. Analytical mass estimation and CAD-based evaluations were used to verify compliance with the mass constraint. The final design remained below the required limit, demonstrating that the deployment subsystem satisfies the mass requirement while maintaining functionality.

Overall, the deployment subsystem design satisfies the primary functional and system-level requirements needed for CORK operation. Through controlled extension, lightweight construction, and simplified actuation, the subsystem provides a reliable method for deploying the reflective film and enabling enhanced solar power generation.

12. *Reflector Subsystem*

The reflector subsystem is responsible for redirecting incident sunlight onto the client spacecraft solar panel to increase its electrical power generation. Its purpose is to provide additional usable solar flux without requiring changes to the existing solar panel architecture. To satisfy the overall mission requirements, the reflector must provide sufficient reflected energy, remain lightweight, and be effective across the wavelengths most relevant to gallium arsenide solar cells. Implementation of the reflector subsystem was therefore driven by three primary goals. First, the reflector must provide enough reflected solar flux to achieve the desired increase in panel performance. Second, it must remain within a constrained mass budget to support spacecraft integration. Third, it must effectively reflect the wavelength range most useful for gallium arsenide solar panels.

To increase the available solar energy to the client panel the reflector will provide an additional 11% of the solar panel's needed solar flux. The 11% increase is made to bring the degraded solar panel back to nominal efficiency levels. The reflector geometry and orientation were designed to redirect additional sunlight onto the solar panel surface at an effective angle. Optical simulation was used to evaluate the reflector's contribution to total solar flux at the panel interface. The reflector area and positioning were selected such that the reflected energy provides at least the required 11% additional solar flux, verifying that the subsystem satisfies the required augmentation performance.

To maintain a lightweight augmentation system, the reflector subsystem will have a total mass of 5 kg or less. To satisfy this requirement, the reflector was designed using lightweight reflective film and a minimal supporting structure to reduce total mass while maintaining sufficient rigidity. Analytical mass estimation and CAD-based mass property evaluations were used to verify compliance with the mass constraint. The final design remained below the required threshold, demonstrating that the reflector subsystem satisfies the allowable spacecraft mass budget.

Aluminized Mylar was selected based on its high optical reflectance across the 400 nm to 1600 nm wavelength range, which corresponds to the useful spectral band for gallium arsenide solar cells [11][12]. Material property

evaluation confirmed that the reflector maintains strong reflectivity throughout this range. This ensures that redirected light remains within wavelengths that can be efficiently converted into electrical power, maintaining compatibility with the client solar panel system.

Overall, the reflector design satisfies the primary performance and system-level requirements needed for SPARK operation. Through adequate solar flux augmentation, low mass, and wavelength compatibility, the reflector provides a feasible method for increasing spacecraft solar power generation without modifying the client panel itself.

I. SPARK Risk Mitigation

SPARK risks are associated with deployment, structural interaction, and material durability. Clamp-induced damage is mitigated by limiting force and distributing loads across padded surfaces. Uneven deployment is prevented using a synchronized motor-driven system. Reflector tearing is mitigated through a carbon fiber cross-hatched backing, increasing strength and resistance to micro-stress damage.

IV. Conclusion

The Mission for Orbital Servicing and Support (MOSS) demonstrates a feasible and scalable approach to extending the operational life of geostationary satellites by directly addressing the primary limitations of propellant depletion and power degradation. By integrating CORK and SPARK, the system enables on-orbit refueling and solar augmentation without requiring modifications to existing spacecraft, ensuring compatibility with current on-orbit assets. Mechanical, fluid, and electrical subsystem analyses validate that the system can safely dock, transfer propellant, and augment power while maintaining structural integrity and operational reliability. Risk mitigation strategies further ensure safe operation through controlled pressure, autonomous shutdown capability, and non-damaging mechanical interfaces. Cost analysis shows that MOSS provides a significant reduction in mission cost compared to full satellite replacement, reinforcing its value as an economically viable solution. Overall, MOSS advances the capability for sustainable space operations by enabling continued use of high-value spacecraft and reducing the need for replacement missions.

Acknowledgments

The authors thank Dr. Swiei Fan for technical guidance, Professor Matthew Haslam for communication support, and Rob Britts for mentorship and sponsorship. The authors also acknowledge Embry-Riddle Aeronautical University and Skyway for their support.

References

[1] Ellery, A., Kreisel, J., and Sommer, B., "The Case for Robotic On-Orbit Servicing of Spacecraft: Spacecraft Reliability Is a Myth," Acta Astronautica, Vol. 63, Nos. 5–6, 2008, pp. 632–648.

[2] Northrop Grumman, "ESPAStar Spacecraft Image," Available at: https://cdn.northropgrumman.com/-/jssmedia/wp-content/uploads/ESPAStar-1-2020.jpg?mw=768&rev=abbee3601058416db65ca20a9bee58fa [accessed Apr. 2026].

[3] Northrop Grumman, "Space Logistics Services," Available at: https://www.northropgrumman.com/what-we-do/space/space-logistics-services [accessed Apr. 2026].

[4] Orbit Fab, "RAFTI: Spacecraft Refueling Interface," Available at: https://www.orbitfab.com/rafti/ [accessed Apr. 2026].

[5] Parker Hannifin Corporation, "O-Ring Selector," Online Engineering Tool, 2024, Available at: https://divapps.parker.com/divapps/oring/ORingSelector?cntry=us/17061&lang=en&region=int [accessed Apr. 2026].

[6] Special Metals Corporation, "INCONEL® Alloy 718: Technical Bulletin SMC-045," Huntington, WV, Sept. 2007, Available at: https://www.specialmetals.com/documents/technical-bulletins/inconel/inconel-alloy-718.pdf [accessed Apr. 2026].

[7] Rolled Alloys, Inc., "Data Sheet – 13-8 Stainless Steel," Temperance, MI, 2011, Available at: https://www.rolledalloys.com/wp-content/uploads/13-8_stainless-steel-data-sheet-rolled-alloys.pdf [accessed Apr. 2026].

[8] Glemco, "Aluminum 6061-T6 Material Information & Specifications," Texas, 2024, Available at: https://www.glemco.com/capabilities/material-expertise/aluminum-6061-t6/ [accessed Apr. 2026].

[9] Han, D. I., Han, C. Y., and Shin, H. D., "Empirical and Computational Performance Prediction for Monopropellant Hydrazine Thruster Employed for Satellite," Journal of Spacecraft and Rockets, Vol. 46, No. 6, 2009, pp. 1186–1195.

[10] Mughari, et al., "Innovative 3D Numerical Study of a Catalyst Bed and Comparison with Previous 2D and Experimental Studies," International Journal of Fluids, Vol. 29, Sept. 2025, Available at: https://doi.org/10.1016/j.ijft.2025.101344.

[11] Bernardes, S., Lameirinhas, R. A. M., Torres, J. P. N., and Fernandes, C. A., "Characterization and Design of Photovoltaic Solar Cells that Absorb Ultraviolet, Visible and Infrared Light," Nanomaterials, Vol. 11, No. 1, 2021, p. 78.

[12] Lugolole, R., and Obwoya, S. K., "The Effect of Thickness of Aluminium Films on Optical Reflectance," Journal of Ceramics, Vol. 2015, No. 1, 2015, p. 213635.